

PFStorer: Personalized Face Restoration and Super-Resolution

Tuomas Varanka^{*1} Tapani Toivonen² Soumya Tripathy² Guoying Zhao¹ Erman Acar²
¹ University of Oulu ² Huawei Finland

tuomas.varanka@oulu.fi

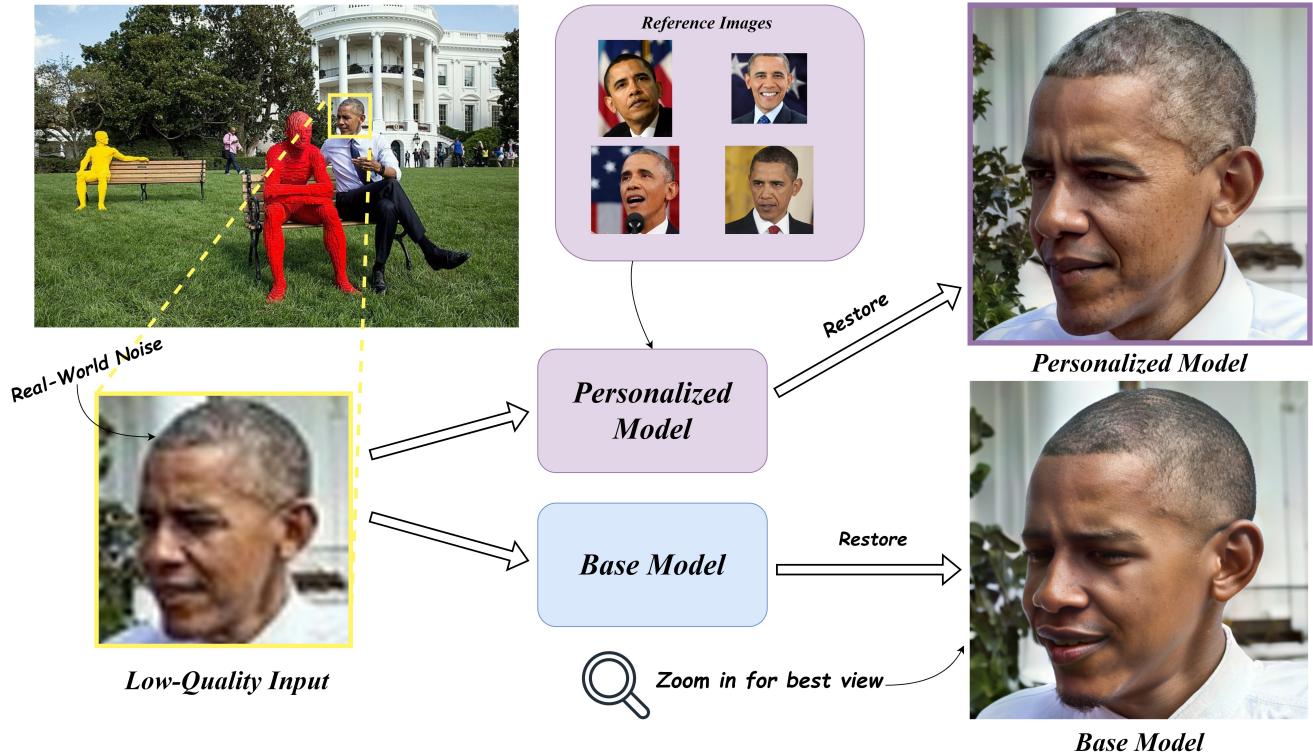


Figure 1. Imagine wanting to restore a photo of yourself, only for the resulting image to not be you, but someone else! By utilizing a few high-quality reference images, we can faithfully restore images with fine-grained details. Best viewed by zooming in.

Abstract

Recent developments in face restoration have achieved remarkable results in producing high-quality and lifelike outputs. The stunning results however often fail to be faithful with respect to the identity of the person as the models lack necessary context. In this paper, we explore the potential of personalized face restoration with diffusion models. In our approach a restoration model is personalized using a few images of the identity, leading to tailored restoration with respect to the identity while retaining fine-grained details. By using independent trainable blocks for personalization, the rich prior of a base restoration model can be exploited to its fullest. To avoid the model relying on parts of identity left in the conditioning low-quality images, a generative regularizer is employed. With a learnable parameter, the model learns to balance between the details generated

based on the input image and the degree of personalization. Moreover, we improve the training pipeline of face restoration models to enable an alignment-free approach. We showcase the robust capabilities of our approach in several real-world scenarios with multiple identities, demonstrating our method’s ability to generate fine-grained details with faithful restoration. In the user study we evaluate the perceptual quality and faithfulness of the generated details, with our method being voted best 61% of the time compared to the second best with 25% of the votes.

1. Introduction

Face restoration aims to recover HQ (high-quality) face images from degraded observations, such as blur, low-resolution, noise and compression artifacts. In real-world scenarios, the task is even more challenging, due to more complex degradations and variations in illumination and

^{*}This research was performed during an internship at Huawei Finland.

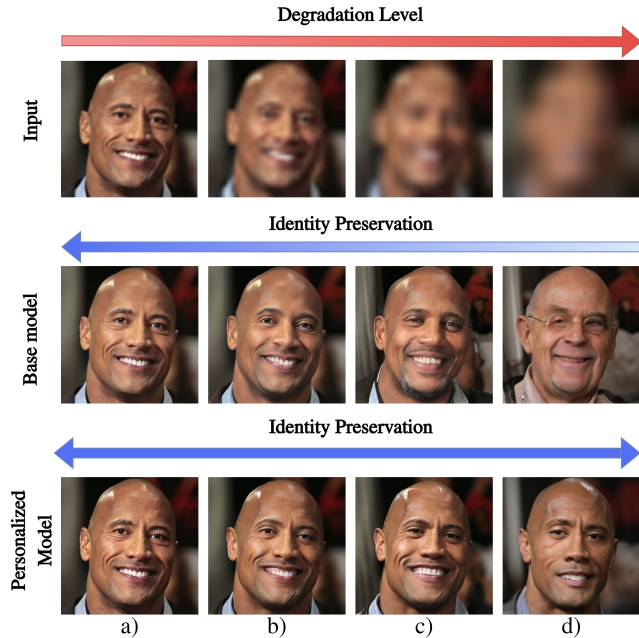


Figure 2. Results under increasing levels of degradation. a) With only minor degradation, both base and personalized model are capable of restoration. b) The base model incorrectly restores fine-grained details such as the nose and skin texture. c) More identity details such as eyes and facial hair are lost. d) Base model outputs a completely different identity, while the personalized model retains details of the identity, even if the semantics are not entirely correct due to the extreme low-quality input image. Best viewed by zooming in.

pose.

Restoration of faces is a highly ill-posed problem with multiple solutions to a given LQ (low-quality) input. Compared to natural images humans are very sensitive to subtle differences with facial images. Even small variations in the shape, size or color of eyes, nose, lips, *etc.*, can cause a shift in the identity of the person, see top and middle row of Fig. 2. Furthermore, if we are familiar with identity of a specific person, we are even more prone to spotting subtle differences. We show an example in Fig. 1. A restoration model needs to not only output a realistic image, but also one that is faithful to the identity of the person.

Recent research on face restoration has seen great progress towards higher visual quality results. Many of the techniques exploit a generative prior such as GAN [3, 8, 40], codebooks [13, 24, 48] or diffusion models [41, 43]. Generative prior methods have been trained under a generative task prior to being modified to restoration models and as a result they are capable of outputting realistic face images. However, often the outputs can be inauthentic as the models lack crucial context about the identity. To combat this, a reference prior has been used [25, 26], which uses a HQ reference image of the same identity, leading in theory to high

fidelity. However, in practice transferring the identity from a reference image is difficult due to differences in pose, illumination and semantics between the LQ and reference image.

To alleviate the ill-posedness of the restoration problem we fully exploit the reference images by creating a *neural representation* of the identity. We propose PFStorer (Personalized Face Restorer) to restore LQ face images while retaining the identity by personalization. Given a few HQ reference images (*e.g.* 3-5 selfies from a photo gallery) a restoration model is fine-tuned to a personalized restoration model. The reference images can have significantly different illumination, pose, expression and do not have to be aligned with the LQ image. Our goal is to personalize a restoration model such that it is able to restore person specific images while producing realistic images and being faithful to the identity.

As opposed to personalized generative models that personalize a generative model, we use a base face restoration model as our foundation. The base model is capable of realistic outputs, however the fidelity may suffer due to the ill-posedness of the task. Our strategy is to perform *personalized restoration* by fine-tuning a base restoration model with a few HQ reference images. However, a naive fine-tuning strategy can destroy the strong existing priors present in the base restoration model. To avoid catastrophic forgetting when performing fine-tuning for personalization, an adapter is used to keep the priors intact. Adapters are trainable blocks that can be used to *adapt* the flow of a model. By freezing the base model and only training the adapter blocks, existing priors can be preserved. To avoid the rapid change of intermediate outputs caused by adapters a learnable parameter is used. The learnable parameter also controls the amount of injection of personalization for different layers of the network, leading to more fine-grained control.

During training, we observe an issue where the model learns to rely too much on the LQ image ignoring the reference images. This is due to the majority of the training samples having low degradation, which can preserve identity information sufficient to restore the face without using the reference images. To alleviate the issue we design a generative regularizer, in which no conditional LQ image is given and the model is forced to generate the identity using only reference images. This approach encourages the model to learn a robust neural representation of the identity, as in generative personalization.

Furthermore, for the base face restoration model we fine-tune a general purpose restoration model on a face dataset to improve its restorative capabilities. During training, instead of resizing all images to a specific size and aligning them, random crops of the face images are used. This has several benefits: 1) The model has access to higher resolution patches. 2) The model is more robust to varying poses.

3) The model is capable of super-resolution through the use of tiling.

We experiment with our technique using both synthetic and real-world data. The user study confirms that our method is able to improve results over previous methods.

2. Related work

Face Restoration Most recent face restoration approaches include a *generative prior*, where the model has been trained in a generative manner *prior* to training it for restoration. GFP-GAN [40] uses the generator of StyleGAN2 [19] that has been trained on facial images to generate high-quality features. More recently, methods such as VQFR [13] and CodeFormer [48] have been using discrete codebooks with vector quantization and adversarial training [9] to “store” high-quality data. Some latest approaches use diffusion models [16] for restoration. DiffFace [43] transforms the LQ input to the manifold of high-quality images with an arbitrary restoration model, which is followed by a forward and backward diffusion, bringing in fine-grained details. DR2 [41] uses a similar approach of first performing forward diffusion, after which backward diffusion is performed with guidance from the matching steps of forward diffusion. Zhao *et al.* [46] note that around 15% of the commonly used training data from FFHQ [18] is not necessarily high-quality. To improve the data quality they propose a two-step training process where after the first step, the training data is enhanced, using the model trained in the first step. Concurrent to our work is DiffBFR [31], which separates identity and texture restoration using cascaded diffusion models. Another concurrent work [5], also emphasizes the ill-posedness of the problem, but goes in the opposite direction to us, encouraging diversity, instead of personalization.

Personalization With the seminal work of DreamBooth [33] personalization of generative models with just a few images was made possible. DreamBooth can generate novel scenes of a specific object or a concept. It achieves this by fine-tuning a text-to-image diffusion model while overwriting a rare text embedding. Several works have since followed [2, 11, 12, 14, 21, 22, 28, 34, 37, 42] that attempt to improve personalization. Custom-Diffusion [21] only fine-tunes the attention layers present in the UNet architecture of StableDiffusion [32], significantly reducing the training time and model size. Perfusion [11] goes further and only does rank-1 updates of the attention layers, while locking the keys of cross-attention layers, significantly reducing compute and memory. ViCo [14] adds image-attention adapters to the cross-attention layers to learn cross-attention between the reference images and predicted image. It also learns a text embedding and applies a regularization using the class-token to avoid overfitting, leading to high-quality

results.

On a high-level similar to our approach is RealFill [36], which personalizes a pre-trained in-painting model to perform authentic in- and out-painting. Both MyStyle [29] and IdentityEncoder [35] first personalize the model and then transform it to perform tasks such as face in-painting, super-resolution and semantic editing. Compared to their approach, we transform a restoration model to a *personalized restoration model* as opposed to transforming a personalized model to a personalized super-resolution model.

Reference-Based Face Restoration Reference-based approaches use reference images from the same identity in the restoration process. GFRNet [23] uses a single reference image and learns a warping between the LQ and reference image. ASFFNet [25] selects the most similar reference image to reduce misalignment and uses adaptive feature fusion for the restoration. DMDNet [26] constructs a dictionary of deep features from important cropped regions (*e.g.*, eyes, nose, mouth). An alignment module is then used to align the features of the input and reference images, resulting in a fusion of the features to the output image. These methods however struggle when the reference image and LQ input are not aligned or not similar enough. Compared to these approaches we learn a neural representation of the identity, enabling more robust restoration.

3. Method

We design a face restoration method capable of generating realistic imagery, while still being faithful to the identity of the person in a given image. We begin by analyzing the situation formally (Sec. 3.1) and conclude that a personal prior is required for faithful reconstruction in certain situations. Next, we present a method (Sec. 3.2) that preserves existing priors by utilizing adapters for personalized face restoration. To further enhance the results a generative regularizer is proposed to enable robust fine-grained restoration. We name this method **PFStorer (ours)**. Beyond personalization (Sec. 3.3), we show simple modifications to the training pipeline of general face restoration methods that enable super-resolution and an alignment-free approach. We refer to this improved restoration model without personalization as the **Base Model**, which is used as a base for personalization. Background for diffusion models and personalization is given in the supplementary material.

3.1. The Need for a Personal Prior

Restoration of low quality images is naturally an ill-posed problem. Assume a degradation function $\mathcal{D} : \mathcal{I} \times \mathbb{R} \rightarrow \mathcal{I}$ that takes in a face image $I \in \mathcal{I}$ and a value of degradation $d \in \mathbb{R}$. A higher degradation value d indicates a higher degraded output image. When d approaches infinity the resulting image will be close to pure noise and restoring the image

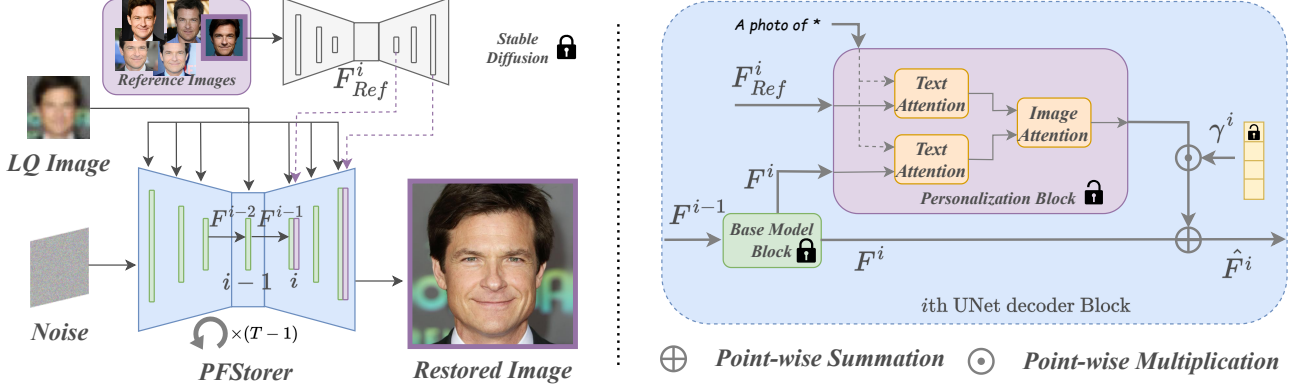


Figure 3. **(Left)** PFStorer restores an image with a diffusion process conditioned on the LQ and the reference image. Base Model blocks are visualized in green and Personalization blocks in purple. StableDiffusion [32] is used to extract features F_{Ref}^i from the reference image. During training the reference image is randomly sampled from a set of reference images for each training iteration. During inference, no reference images are required as the identity is learned in the personalization blocks as a neural representation. **(Right)** i th UNet block containing the Base Model Block [38] and Personalization Block [14]. The Base Model Blocks contain the normal Stable Diffusion blocks with SFT (spatial feature transformation) [39] blocks from StableSR [38]. After the Base Model block, the intermediate features F^i go to a trainable Personalization Block, which contains cross-attention between the text-embedding and reference image features F_{Ref}^i . A learnable adapter vector γ^i balances the contribution between the base model and personalization.

faithfully is no longer possible, $id(\mathcal{R}(\mathcal{D}(I; d))) \neq id(I)$, where id is a function that returns the identity of a face image and \mathcal{R} is a restoration model. There exists a value $d_f < \infty$ after which faithful restoration is no longer possible. However, with additional personal prior p_{id} the restoration can be made faithfully:

$$id(\mathcal{R}(\mathcal{D}(I; d_f); p_{id})) = id(I), \quad (1)$$

as p_{id} is unchanged with any value of degradation d . In this paper the personal prior p_{id} is learned from a set of reference images using a diffusion model.

3.2. Personalized Face Restoration

The main idea is to use high-quality images of an individual in aid when restoring LQ images. We start with a restoration model, which is fine-tuned with a personalization technique using the reference images. The personalization is performed for each individual once, after which it can be used for inference as many times as wanted. In essence, the model is trained to add personal details, when the base restoration model is insufficient, due to the ill-posed nature of the problem. The architecture of the model can be seen from Fig. 3.

During the personalization fine-tuning, the model takes as input a synthesized LQ image I_{LQ} and a reference image I_{Ref} sampled from the set of reference images $\{I_{Ref}^k\}$. A modified diffusion model loss

$$\mathcal{L}_{Diff} = \mathbb{E}_{z_t, t, I_{LQ}, I_{Ref}, \epsilon} \|\epsilon - \epsilon_\theta(z_t, c, I_{LQ}, I_{Ref})\|_2, \quad (2)$$

with the addition of the LQ and reference image, is used. Here ϵ_θ is the diffusion model, z_t the latent code at time t ,

c the conditioning text embedding and ϵ the sampled noise from an Isotropic Gaussian distribution.

Personalization We initially attempt to fine-tune with prior-preservation regularization [33], but find that it fails to properly capture the fine-grained identity details as well as diminishes the results from restoration due to modifying existing priors. This motivates the need for preserving the priors completely, leaving the priors untouched. Therefore, we prefer to utilize adapter blocks, which do not modify the existing priors at all, retaining their rich abilities to restore and generate. In order to implement this, we employ text and image cross-attentions between the learnable text-embedding [10], reference image features F_{Ref}^i and intermediate restored image features F^i of the layer i , as used similarly in [14] and shown on Fig. 3 right. The reference image features F_{Ref}^i are obtained from a frozen StableDiffusion [32], in practice they are fed through part of the Base Model in same batch as the LQ image. We refer to this as the *Personalization Block* (see Fig. 3 right).

Controlled Adaptation The simple addition of the personalization block however results in distorted outputs. This is due to the sudden additional data being added to the intermediate features of the Base Model from the personalization block. In order to avoid the personalization block from changing the outputs too much, a learnable vector $\gamma = \mathbf{0}$ can be used to initialize the outputs from the adapter, as in [4]. To further control the effect of personalization we introduce separate γ for each personalization block applied at different resolution of PFStorer. Mathematically, each layer’s output can be expressed as:



Figure 4. 20x Super-resolution of a low-quality image. Super-resolution for images larger than 512×512 using a tiling approach from [38]. Image edited from Vecteezy.com.

$$\hat{F}^i = F^i + \gamma^i \odot \text{Personalization-Block}(F^i, F_{ref}^i), \quad (3)$$

where Personalization-Block is the adapter, consisting of cross-attentions as shown on right of Fig. 3.

Generative Regularization Compared to personalized generative models our personalized restoration model has one additional signal, the low-quality image I_{LQ} . It guides the general structure of the restoration output and it may contain some information from the identity depending on the severity of the degradation. During training, the additional input can make the task of outputting personalized restored images easier, but it can also introduce shortcuts for the model as the model can rely on information from the additional input. This leaking of identity information from the input can lead to the model not fully learning a representation of the identity during training, hence leading to poor performance on difficult unseen cases, *e.g.* atmospheric turbulence.

To mitigate the above issue, we propose a generative regularizer that encourages the model to learn a more robust identity representation. A regularizing loss

$$\mathcal{L}_{Gen} = \mathbb{E}_{z,t,I_{LQ},I_{Ref},\epsilon} \|\epsilon - \epsilon_{\theta}(z_t, c, \emptyset, I_{Ref})\|_2. \quad (4)$$

is added to the original training loss, where a null input \emptyset is given as the conditioning LQ image. This forces the model to fully hallucinate the identity without any help from a conditioning image, encouraging a more robust representation of the identity. The final loss is then

$$\mathcal{L} = \mathcal{L}_{Diff} + \lambda_{Gen}\mathcal{L}_{Gen} + \lambda_{Pers}\mathcal{L}_{Pers} \quad (5)$$

where λ_{Gen} controls the weight of the generative term and $\lambda_{Pers}\mathcal{L}_{Pers}$ regularizes the cross-attention maps for the learnable text embedding token, which enforces personalization [14] (see the supplementary for \mathcal{L}_{Pers}). The trainable parameters θ from ϵ_{θ} consist of the personalization blocks and their accompanying vectors γ^i .

3.3. Improving Face Restoration Diffusion Models

To integrate personalization into a restoration model, we first need a strong base restoration model. We train our model with the facial dataset FFHQ using the steps described below, which is initialized from the pre-trained StableSR [38]. We refer to the trained model as **Base Model**, as it has not been personalized to any specific person.

Existing Priors Many recent face restoration methods have used generative priors [40, 48]. We go further, and start our training on face images with a restoration model

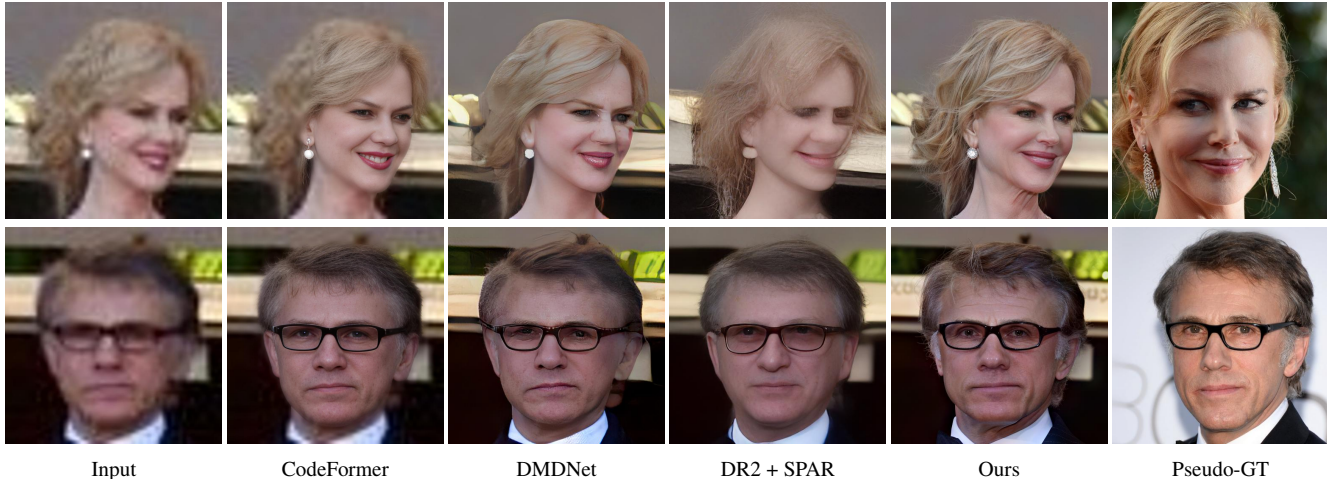


Figure 5. Qualitative comparison with state-of-the-art restoration models on real-world images. Images from Wikimedia Commons.

pre-trained on generic natural images, namely StableSR [38]. As the model is not trained from scratch on a new task, the training time is decreased and the model is more robust.

Alignment Free Approach Cropping and alignment is commonly used in face processing for standardizing input. However, delicate cropping and alignment using facial landmarks is prone to errors when face detection models fail. This is especially true in real world images. To avoid such approach we train our technique with a combination of random crops and resizing, following the training strategy of [38]. The random crops make the model more robust while also providing higher resolution inputs as details are not lost in the resizing operation.

Synthetic Noise Generation In order to generate LQ images for training, most previous face restoration approaches have used a simple first-order degradation that may not encompass all noises present in real-world images. We use a second order noise model from [38], ISP model from [44] and add motion blur and median blur to better simulate real-world conditions. As noted in [46], given a high-quality input, a restoration model should not lose details in the restoration process. We enforce this by directly feeding the high-quality input as is with a probability of p_{HQ} , which is set to a low value of 0.03 in all of our experiments.

4. Experiments

Datasets For evaluation we use Celeb-Ref [26] and real-world images collected from the internet. Due to the large computational cost of diffusion models we choose a small subsection of the original Celeb-Ref. For synthetic data evaluation that contains the ground truth, we randomly choose 20 identities with at least 10 images each, for a total of 342 images. For each identity we reserve 5 images for the

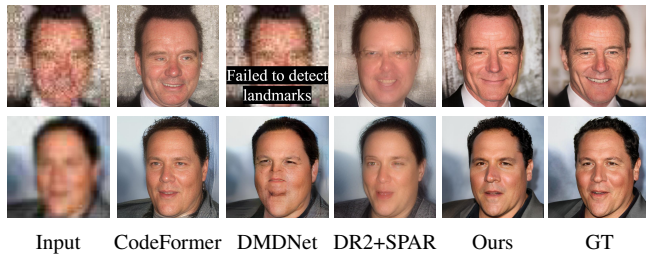


Figure 6. Qualitative comparison with state-of-the-art restoration models on Celeb-Ref dataset [26] with heavy synthetic degradation. Best viewed zoomed in.

personalization, leaving a total 242 images for the testing. We further use two variations, *light* and *heavy* degradation sets, see the supplementary for details. For real-world data we again randomly choose 20 identities from Celeb-Ref, reverse search the identities using LAION-5B-KNN [1] and collect one image for each identity from online. We focus on high-quality images, where the subject is far away and/or out of focus and/or with poor illumination to best simulate real-world applications.

Baselines CodeFormer [48] is state-of-the-art technique for face restoration and it uses a codebook. DR2 [41] is based on a diffusion model and is meant for extreme degradations. For DR2, we use the provided SPAR enhancer and empirically find the optimal hyperparameters. DMDNet [26] is state-of-the-art method for reference-based face restoration, for which we use the same set of 5 reference images as for the proposed method.

Evaluation Metrics For quantitative evaluation we use PSNR, SSIM, LPIPS [45], MUSIQ (KonIQ) [20], LMSE (Landmark MSE) [47], and ID (cosine similarity with ArcFace [7]) as metrics.

Settings For methods that use reference images, 5 images are randomly sampled. For PFStorer, the personalization

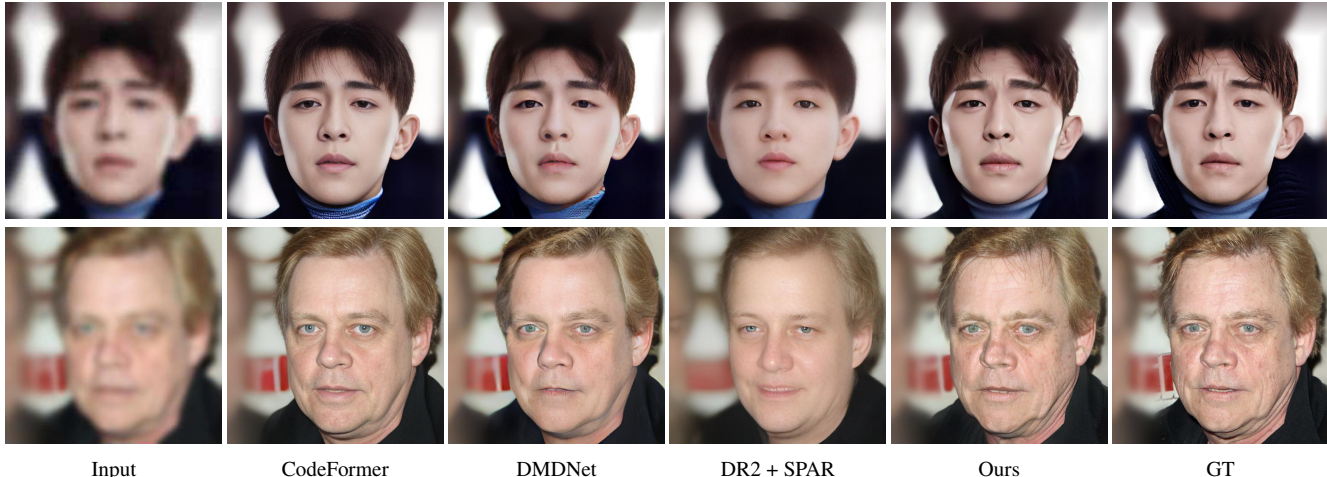


Figure 7. Qualitative comparison with state-of-the-art restoration models on Celeb-Ref dataset [26] with light synthetic degradation.

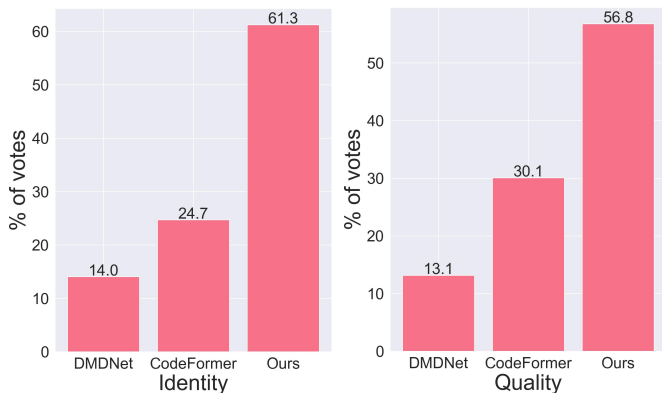


Figure 8. User study results.

fine-tuning is done for 500 iterations, which corresponds to 10 minutes on a single A100. For all of our experiments we set the same settings, hyperparameters and a single seed. For detailed experimental settings see the supplementary material.

4.1. Comparisons

Qualitative To evaluate the effectiveness of the proposed method we show visual results in Figs. 4 to 7, for real-world, low-quality images collected from real-world, corrupted with heavy and light degradations. For the real-world sample we provide a pseudo-GT that can be used to compare with the identity. It can be observed from Fig. 5 that the baseline methods fail in preserving the identity and producing a high-quality image. Despite the difficult case on first row Fig. 5, where the head pose is atypical, the proposed method is able to restore the image faithfully, thanks to the learned representation of the identity. Figure 6 shows examples with heavy synthetic degradation. Even under heavy degradation the proposed method is able to restore the image faithfully, while other methods struggle with re-

taining the identity and outputting a realistic image. Under light degradation in Fig. 7, CodeFormer is able to output a high-quality image while mostly retaining the identity. Our method is able to retain even small details such as the wrinkles and skin texture.

Quantitative Quantitative results on the heavily degraded images can be seen from Tab. 1. The pixel-wise metrics PSNR and SSIM as well as the perceptual metric LPIPS have relatively similar values across the best performing methods, with slight differences. Notably, the big difference is in the ID metric, where the proposed method obtains a similarity of 57.18%, almost 20 percentage points higher than the next best performing method. This result showcases the benefit of personalization for retaining identity features. Another major improvement can be seen in the LMSE with almost half the error compared to CodeFormer. This is due to the combination of a strong base model and personalization. See supplementary for the real-world and lightly degraded samples.

Table 1. Quantitative results for images with heavy degradation. Red indicates the best and blue indicates the second best. Ref indicates whether the model uses reference images

Methods	Ref	PSNR \uparrow	SSIM \uparrow	LPIPS \downarrow	MUSIQ \uparrow	LMSE \downarrow	ID \uparrow
Input		22.56	0.719	0.615	58.83	80.98	21.85
DMDNet [26]	✓	22.64	0.684	0.491	47.17	89.26	29.51
DR2 + SPAR [41]		22.17	0.701	0.449	47.36	40.82	30.01
CodeFormer [48]		22.26	0.642	0.422	60.92	33.34	38.33
PFStorer (Ours)	✓	22.62	0.679	0.414	64.04	18.37	57.18
GT		∞	1	0	62.37	0	100

User Study As the quantitative metrics are not fully able to capture the nuances of human preferred perceptual quality, a user study is conducted. We use all three partitions of the data. We randomly pick 100 images. To attain statistical significance we recruit 40 users, following [30]. With two questions we have a total of 8000 answers from users. We compare our method to only CodeFormer and DMDNet, as

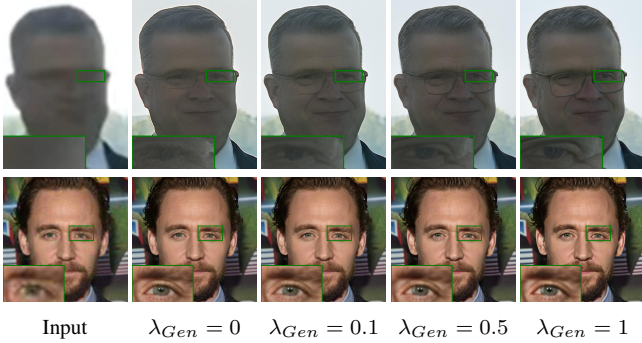


Figure 9. (Top) In the presence of heavy degradation a larger λ_{Gen} is able to improve results. (Bottom) With minor degradation, a larger λ_{Gen} can deteriorate results.

DR2 often produces low-quality images. We ask users to choose between the best image in terms of quality and identity with respect to a reference image.

The results are shown in Fig. 8. Our method obtains the highest number of votes in both perceived identity and quality. Our method is especially good in capturing the identity, gaining 36.6 percentage points over the next best method, CodeFormer. This result resonates with both the qualitative results and quantitative metrics.

4.2. Further analysis

Personalization Table 2 demonstrates the improvements of the proposed method for personalization. Without personalization, the Base Model with the improved training mechanism is able to improve over StableSR [38] in all metrics. However, the results fall behind largely when personalization is added. Base Model + DreamBooth [33] and Base Model + ViCo [14] attain similar metrics, however a drop in the PSNR value even below StableSR [38] and the increase in LMSE compared to Base Model, signifies how fine-tuning the whole model can hurt the existing priors. For a fair comparison Base + ViCo also contains generative regularization and other proposed training method proposed and only lacks the learnable γ compared to PFStorer. The γ provides important balance over the personalized and restored features.

Table 2. Quantitative results for different personalization methods on the heavy portion. Red indicates the best and blue indicates the second best

Methods	Ref	PSNR \uparrow	SSIM \uparrow	LPIPS \downarrow	MUSIQ \uparrow	LMSE \downarrow	ID \uparrow
Input		22.56	0.719	0.615	58.83	80.98	21.85
StableSR [38]		21.68	0.601	0.605	38.55	93.82	22.87
Base Model		22.15	0.661	0.449	64.33	32.83	33.90
Base + DreamBooth [33]	✓	21.13	0.659	0.487	62.65	37.48	52.72
Base + ViCo [14]	✓	22.14	0.664	0.423	65.23	20.26	53.92
PFStorer (Ours)	✓	22.62	0.679	0.414	64.04	18.37	57.18
GT		∞	1	0	62.37	0	100

Alignment-Free Training and Existing Priors An immediate benefit to our landmark- and alignment-free ap-

proach is that it can be run even when the landmark model fails, as can be seen from the top row of Fig. 6. Furthermore, due to the existing priors of the Base Model, the model is able to restore details from the full head and not only the face, see the result from CodeFormer from Fig. 5 top.

Generative Regularization Figure 9 showcases results with different values of the weight λ_{Gen} of generative regularization. A larger λ_{Gen} encourages more hallucination, which is beneficial for unseen cases, while a smaller λ_{Gen} focuses more on the restoration. To balance the effects we use a default $\lambda_{Gen} = 0.1$ for all of our experiments based on empirical observations.

4.3. Limitations

We show an example of a limitation in Fig. 10. The output is faithful to the given reference images, hence if there are changes in the appearance between references and the input the result may be unwanted. As the model is based on Stable Diffusion it inherits its limitations of slow sampling speed and occasional unwanted artifacts and hallucinations due to the stochasticity. As a possible solution to stochasticity, concurrent work [6] guides the model towards visually appealing results.



Figure 10. The output is as accurate as the given reference images are.

5. Conclusions

In this work, we introduce the use of *personalization* for the task of face restoration, where a restoration model is personalized using a few images of a person. We postulate that the problem of face restoration is an ill-posed problem and requires the use of a personal prior for faithful results. We propose the use of a personalization adapter that preserves existing priors of the base restoration model. To enhance the training generative regularization is designed. We showcase our method’s abilities through qualitative, quantitative and a user study.

Acknowledgements This work was supported by the Research Council of Finland Academy Professor project EmotionAI (grants 336116, 345122), ICT 2023 project TrustFace (grant 345948), the University of Oulu & Research Council of Finland Profi 7 (grant 352788), and by Infotech Oulu.

References

- [1] LAION AI. Laion-knn api. <https://rom1504.github.io/clip-retrieval/?back=https%3A%2F%2Fknn.laion.ai&index=laion5B-H-14&useMclip=false>. Accessed 10-10-2023. 6
- [2] Yuval Alaluf, Elad Richardson, Gal Metzger, and Daniel Cohen-Or. A neural space-time representation for text-to-image personalization, 2023. 3
- [3] Chaofeng Chen, Xiaoming Li, Lingbo Yang, Xianhui Lin, Lei Zhang, and Kwan-Yee K Wong. Progressive semantic-aware style transformation for blind face restoration. In *Proceedings of the IEEE/CVF conference on computer vision and pattern recognition*, pages 11896–11905, 2021. 2
- [4] Zhe Chen, Yuchen Duan, Wenhai Wang, Junjun He, Tong Lu, Jifeng Dai, and Yu Qiao. Vision transformer adapter for dense predictions, 2023. 4
- [5] Noa Cohen, Hila Manor, Yuval Bahat, and Tomer Michaeli. From posterior sampling to meaningful diversity in image restoration, 2023. 3
- [6] Xiaoliang Dai, Ji Hou, Chih-Yao Ma, Sam Tsai, Jiali Wang, Rui Wang, Peizhao Zhang, Simon Vandenhende, Xiaofang Wang, Abhimanyu Dubey, et al. Emu: Enhancing image generation models using photogenic needles in a haystack. *arXiv preprint arXiv:2309.15807*, 2023. 8
- [7] Jiankang Deng, Jia Guo, Niannan Xue, and Stefanos Zafeiriou. Arcface: Additive angular margin loss for deep face recognition. In *Proceedings of the IEEE/CVF conference on computer vision and pattern recognition*, pages 4690–4699, 2019. 6, 14
- [8] Berk Dogan, Shuhang Gu, and Radu Timofte. Exemplar guided face image super-resolution without facial landmarks. In *Proceedings of the IEEE/CVF conference on computer vision and pattern recognition workshops*, pages 0–0, 2019. 2
- [9] Patrick Esser, Robin Rombach, and Bjorn Ommer. Taming transformers for high-resolution image synthesis. In *Proceedings of the IEEE/CVF conference on computer vision and pattern recognition*, pages 12873–12883, 2021. 3
- [10] Rinon Gal, Yuval Alaluf, Yuval Atzmon, Or Patashnik, Amit H Bermano, Gal Chechik, and Daniel Cohen-Or. An image is worth one word: Personalizing text-to-image generation using textual inversion. *arXiv preprint arXiv:2208.01618*, 2022. 4, 11
- [11] Rinon Gal, Moab Arar, Yuval Atzmon, Amit H Bermano, Gal Chechik, and Daniel Cohen-Or. Encoder-based domain tuning for fast personalization of text-to-image models. *ACM Transactions on Graphics (TOG)*, 42(4):1–13, 2023. 3
- [12] Jing Gu, Yilin Wang, Nanxuan Zhao, Tsu-Jui Fu, Wei Xiong, Qing Liu, Zhifei Zhang, He Zhang, Jianming Zhang, Hyun-Joon Jung, et al. Photoswap: Personalized subject swapping in images. *arXiv preprint arXiv:2305.18286*, 2023. 3
- [13] Yuchao Gu, Xintao Wang, Liangbin Xie, Chao Dong, Gen Li, Ying Shan, and Ming-Ming Cheng. Vqfr: Blind face restoration with vector-quantized dictionary and parallel decoder. In *European Conference on Computer Vision*, pages 126–143. Springer, 2022. 2, 3
- [14] Shaozhe Hao, Kai Han, Shihao Zhao, and Kwan-Yee K Wong. Vico: Detail-preserving visual condition for personalized text-to-image generation. *arXiv preprint arXiv:2306.00971*, 2023. 3, 4, 5, 8, 11
- [15] Jonathan Ho and Tim Salimans. Classifier-free diffusion guidance. *arXiv preprint arXiv:2207.12598*, 2022. 13
- [16] Jonathan Ho, Ajay Jain, and Pieter Abbeel. Denoising diffusion probabilistic models. *Advances in neural information processing systems*, 33:6840–6851, 2020. 3, 11, 12
- [17] Gary B Huang, Marwan Mattar, Tamara Berg, and Eric Learned-Miller. Labeled faces in the wild: A database for studying face recognition in unconstrained environments. In *Workshop on faces in 'Real-Life' Images: detection, alignment, and recognition*, 2008. 15, 21
- [18] Tero Karras, Samuli Laine, Miika Aittala, Janne Hellsten, Jaakko Lehtinen, and Timo Aila. Analyzing and improving the image quality of stylegan. In *Proceedings of the IEEE/CVF conference on computer vision and pattern recognition*, pages 8110–8119, 2020. 3, 14
- [19] Tero Karras, Samuli Laine, Miika Aittala, Janne Hellsten, Jaakko Lehtinen, and Timo Aila. Analyzing and improving the image quality of stylegan. In *Proceedings of the IEEE/CVF conference on computer vision and pattern recognition*, pages 8110–8119, 2020. 3
- [20] Junjie Ke, Qifei Wang, Yilin Wang, Peyman Milanfar, and Feng Yang. Musiq: Multi-scale image quality transformer. In *Proceedings of the IEEE/CVF International Conference on Computer Vision*, pages 5148–5157, 2021. 6, 14
- [21] Nupur Kumari, Bingliang Zhang, Richard Zhang, Eli Shechtman, and Jun-Yan Zhu. Multi-concept customization of text-to-image diffusion. In *Proceedings of the IEEE/CVF Conference on Computer Vision and Pattern Recognition*, pages 1931–1941, 2023. 3
- [22] Dongxu Li, Junnan Li, and Steven CH Hoi. Blip-diffusion: Pre-trained subject representation for controllable text-to-image generation and editing. *arXiv preprint arXiv:2305.14720*, 2023. 3
- [23] Xiaoming Li, Ming Liu, Yuting Ye, Wangmeng Zuo, Liang Lin, and Ruigang Yang. Learning warped guidance for blind face restoration. In *Proceedings of the European conference on computer vision (ECCV)*, pages 272–289, 2018. 3
- [24] Xiaoming Li, Chaofeng Chen, Shangchen Zhou, Xianhui Lin, Wangmeng Zuo, and Lei Zhang. Blind face restoration via deep multi-scale component dictionaries. In *European conference on computer vision*, pages 399–415. Springer, 2020. 2
- [25] Xiaoming Li, Wenyu Li, Dongwei Ren, Hongzhi Zhang, Meng Wang, and Wangmeng Zuo. Enhanced blind face restoration with multi-exemplar images and adaptive spatial feature fusion. In *Proceedings of the IEEE/CVF Conference on Computer Vision and Pattern Recognition*, pages 2706–2715, 2020. 2, 3
- [26] Xiaoming Li, Shiguang Zhang, Shangchen Zhou, Lei Zhang, and Wangmeng Zuo. Learning dual memory dictionaries for blind face restoration. *IEEE Transactions on Pattern Analysis and Machine Intelligence*, 45(5):5904–5917, 2022. 2, 3, 6, 7, 14, 15, 16, 17, 18

- [27] Ziwei Liu, Ping Luo, Xiaogang Wang, and Xiaoou Tang. Deep learning face attributes in the wild. In *Proceedings of the IEEE international conference on computer vision*, pages 3730–3738, 2015. 15, 21
- [28] Jian Ma, Junhao Liang, Chen Chen, and Haonan Lu. Subject-diffusion: Open domain personalized text-to-image generation without test-time fine-tuning. *arXiv preprint arXiv:2307.11410*, 2023. 3
- [29] Yotam Nitzan, Kfir Aberman, Qiuwei He, Orly Liba, Michal Yarom, Yossi Gandelsman, Inbar Mosseri, Yael Pritch, and Daniel Cohen-Or. Mystyle: A personalized generative prior. *ACM Transactions on Graphics (TOG)*, 41(6):1–10, 2022. 3
- [30] Mayu Otani, Riku Togashi, Yu Sawai, Ryosuke Ishigami, Yuta Nakashima, Esa Rahtu, Janne Heikkilä, and Shin’ichi Satoh. Toward verifiable and reproducible human evaluation for text-to-image generation. In *Proceedings of the IEEE/CVF Conference on Computer Vision and Pattern Recognition*, pages 14277–14286, 2023. 7, 12
- [31] Xinmin Qiu, Congying Han, ZiCheng Zhang, Bonan Li, Tiande Guo, and Xuecheng Nie. Diffbfr: Bootstrapping diffusion model towards blind face restoration. *arXiv preprint arXiv:2305.04517*, 2023. 3
- [32] Robin Rombach, Andreas Blattmann, Dominik Lorenz, Patrick Esser, and Björn Ommer. High-resolution image synthesis with latent diffusion models. In *Proceedings of the IEEE/CVF conference on computer vision and pattern recognition*, pages 10684–10695, 2022. 3, 4, 11
- [33] Nataniel Ruiz, Yuanzhen Li, Varun Jampani, Yael Pritch, Michael Rubinstein, and Kfir Aberman. Dreambooth: Fine tuning text-to-image diffusion models for subject-driven generation. In *Proceedings of the IEEE/CVF Conference on Computer Vision and Pattern Recognition*, pages 22500–22510, 2023. 3, 4, 8, 14
- [34] Nataniel Ruiz, Yuanzhen Li, Varun Jampani, Wei Wei, Tingbo Hou, Yael Pritch, Neal Wadhwa, Michael Rubinstein, and Kfir Aberman. Hyperdreambooth: Hypernetworks for fast personalization of text-to-image models. *arXiv preprint arXiv:2307.06949*, 2023. 3
- [35] Yu-Chuan Su, Kelvin CK Chan, Yandong Li, Yang Zhao, Han Zhang, Boqing Gong, Huisheng Wang, and Xuhui Jia. Identity encoder for personalized diffusion. *arXiv preprint arXiv:2304.07429*, 2023. 3
- [36] Luming Tang, Nataniel Ruiz, Qinghao Chu, Yuanzhen Li, Aleksander Holynski, David E. Jacobs, Bharath Hariharan, Yael Pritch, Neal Wadhwa, Kfir Aberman, and Michael Rubinstein. Realfill: Reference-driven generation for authentic image completion, 2023. 3
- [37] Yoad Tewel, Rinon Gal, Gal Chechik, and Yuval Atzmon. Key-locked rank one editing for text-to-image personalization. In *ACM SIGGRAPH 2023 Conference Proceedings*, pages 1–11, 2023. 3
- [38] Jianyi Wang, Zongsheng Yue, Shangchen Zhou, Kelvin C. K. Chan, and Chen Change Loy. Exploiting diffusion prior for real-world image super-resolution, 2023. 4, 5, 6, 8, 11, 12, 13, 14
- [39] Xintao Wang, Ke Yu, Chao Dong, and Chen Change Loy. Recovering realistic texture in image super-resolution by deep spatial feature transform. In *Proceedings of the IEEE conference on computer vision and pattern recognition*, pages 606–615, 2018. 4
- [40] Xintao Wang, Yu Li, Honglun Zhang, and Ying Shan. Towards real-world blind face restoration with generative facial prior. In *Proceedings of the IEEE/CVF conference on computer vision and pattern recognition*, pages 9168–9178, 2021. 2, 3, 5, 15, 21
- [41] Zhixin Wang, Ziying Zhang, Xiaoyun Zhang, Huangjie Zheng, Mingyuan Zhou, Ya Zhang, and Yanfeng Wang. Dr2: Diffusion-based robust degradation remover for blind face restoration. In *Proceedings of the IEEE/CVF Conference on Computer Vision and Pattern Recognition*, pages 1704–1713, 2023. 2, 3, 6, 7, 12, 14, 15
- [42] Guangxuan Xiao, Tianwei Yin, William T Freeman, Frédéric Durand, and Song Han. Fastcomposer: Tuning-free multi-subject image generation with localized attention. *arXiv preprint arXiv:2305.10431*, 2023. 3
- [43] Zongsheng Yue and Chen Change Loy. Difface: Blind face restoration with diffused error contraction. *arXiv preprint arXiv:2212.06512*, 2022. 2, 3
- [44] Kai Zhang, Yawei Li, Jingyun Liang, Jiezhang Cao, Yulun Zhang, Hao Tang, Deng-Ping Fan, Radu Timofte, and Luc Van Gool. Practical blind image denoising via swin-conv-UNet and data synthesis. *Machine Intelligence Research*, 2023. 6, 12
- [45] Richard Zhang, Phillip Isola, Alexei A Efros, Eli Shechtman, and Oliver Wang. The unreasonable effectiveness of deep features as a perceptual metric. In *Proceedings of the IEEE conference on computer vision and pattern recognition*, pages 586–595, 2018. 6
- [46] Yang Zhao, Tingbo Hou, Yu-Chuan Su, Xuhui Jia, Yandong Li, and Matthias Grundmann. Towards authentic face restoration with iterative diffusion models and beyond. In *Proceedings of the IEEE/CVF International Conference on Computer Vision (ICCV)*, pages 7312–7322, 2023. 3, 6
- [47] Yinglin Zheng, Hao Yang, Ting Zhang, Jianmin Bao, Dongdong Chen, Yangyu Huang, Lu Yuan, Dong Chen, Ming Zeng, and Fang Wen. General facial representation learning in a visual-linguistic manner. In *Proceedings of the IEEE/CVF Conference on Computer Vision and Pattern Recognition*, pages 18697–18709, 2022. 6, 12
- [48] Shangchen Zhou, Kelvin Chan, Chongyi Li, and Chen Change Loy. Towards robust blind face restoration with codebook lookup transformer. *Advances in Neural Information Processing Systems*, 35:30599–30611, 2022. 2, 3, 5, 6, 7, 14, 15, 21

PFStorer: Personalized Face Restoration and Super-Resolution

Supplementary Material

This supplementary material contains the following sections. First, background is provided for the used models. Next, further details of the user study are provided. Then, full experimental details and additional experiments of the personalized model are shown. Finally, the training details and further experiments of the non-personalized base restoration model are discussed. As the last section, societal impact is discussed.

Background

In this section we provide sufficient background to keep the paper self-sustained. We first introduce latent diffusion models, namely Stable Diffusion [32], as both the used methods, StableSR [38] and ViCo [14] are based off of it. Next we provide further details of the base model, StableSR and the personalization technique ViCo.

Latent Diffusion Models As oppose to diffusion models [16], LDMs [32] (latent diffusion models) perform the diffusion steps in a latent space. In Stable Diffusion [32] an encoder \mathcal{E} is first trained to map input images $x \in \mathbb{R}^{H \times W \times 3}$ to a latent code $z = \mathcal{E}(x) \in \mathbb{R}^{(H/8) \times (W/8) \times 4}$, which can be approximately reconstructed with a decoder \mathcal{D} . The diffusion forward and backward steps are then performed within the latent space. To perform conditional generation using text y , it is first transformed to an embedding $c(y)$ with a text embedder. The training loss is then given by:

$$\mathcal{L} = \mathbb{E}_{z \sim \mathcal{E}(x), y, \epsilon \sim \mathcal{N}(0,1), t} [\|\epsilon - \epsilon_\theta(z_t, c(y), t)\|_2^2]. \quad (6)$$

Above, at timestep t the diffusion model $\epsilon_{t\theta}$ denoises the added noise from z_t conditioned on the text embedding $c(y)$ and the timestep t . After training the model can be used to generate images with a text prompt y and starting from a $z_t \sim \mathcal{N}(0, 1)$ iteratively until all noise is removed at $t = 0$.

StableSR To exploit the rich generative prior in Stable Diffusion [32] for image restoration, StableSR [38] uses conditioning of low-quality images. The entire Stable Diffusion is kept frozen, while a time-aware encoder and spatial feature transformations are added as adapters to condition the low-quality images. The encoder takes in a low-quality image and the current time-step of the diffusion model and outputs feature maps at different resolutions, corresponding to the ones in Stable Diffusion’s UNet. The features are then fed through spatial feature transforms and added to the output of the original UNet layer’s intermediate outputs.

The model is trained on high-quality generic natural images of 2k and 8k resolutions, which are randomly cropped

to 512×512 . This training enables the use of arbitrary size super-resolution using aggregation sampling. Here, the input is split to overlapping tiles, which are processed by the model independently. To avoid border artifacts a Gaussian kernel is used for the fusion of the tiles.

ViCo For efficient and accurate personalization, ViCo [14] also uses Stable Diffusion as its base. Similarly to StableSR, ViCo keeps the entire Stable Diffusion frozen. Only added adapter blocks and a single text-embedding are trained. Similar to [10], a text-embedding is made learnable that can be associated with the subject. Additionally, image cross-attention adapters are added to four blocks of the UNet. These cross-attention layers take the current time-step’s intermediate result and the intermediate features of a reference image, which has also gone through the UNet. To enhance the result, a mask is used to ignore the background. The mask is obtained from an attention map $A = \text{softmax}\left(\frac{QK^T}{\sqrt{d_k}}\right)$, which is a product of the reference image and the text-embedding. A regularizer

$$\mathcal{L}_{Pers} = \|A_\star / \max(A_\star) - A_{EOT} / \max(A_{EOT})\|_2^2, \quad (7)$$

where A_\star are the similarity logits corresponding to the learnable token of the text-embedding and A_{EOT} is the end-of-text token, is used to avoid overfitting. The end-of-text token $\langle \text{EOT} \rangle$ captures a global representation, which retains good semantics of the personalizable object through training.

User Study Details

From the light and heavy partitions we randomly select two images for each identity. From the real data, we select all of the images. In total we have $20 \times 2 + 20 \times 2 + 20 \times 1 = 100$ images. With 40 users and two tasks we have a total of 8000 unique answers. As identifying fine-grained details of an identity, especially not a familiar one, can be difficult, we chose four images from each identity (light and heavy). This way the users can get more accustomed to the identities and make more accurate evaluations for the similarity of the identity features.

To ensure that the users are being accurate with their annotations, we use five control tasks. Here a ground-truth image is paired with extremely poor quality images. If the user fails in these tasks, their annotations are likely to be inaccurate and their results can be potentially invalidated. To avoid biases with users always choosing A, B or C, we randomly shuffle the model’s positions.

Figure 11 displays the user interface used for the study. Users have to read the full instructions before taking the

Instructions: Choose which option, A, B or C, has the best quality and identity

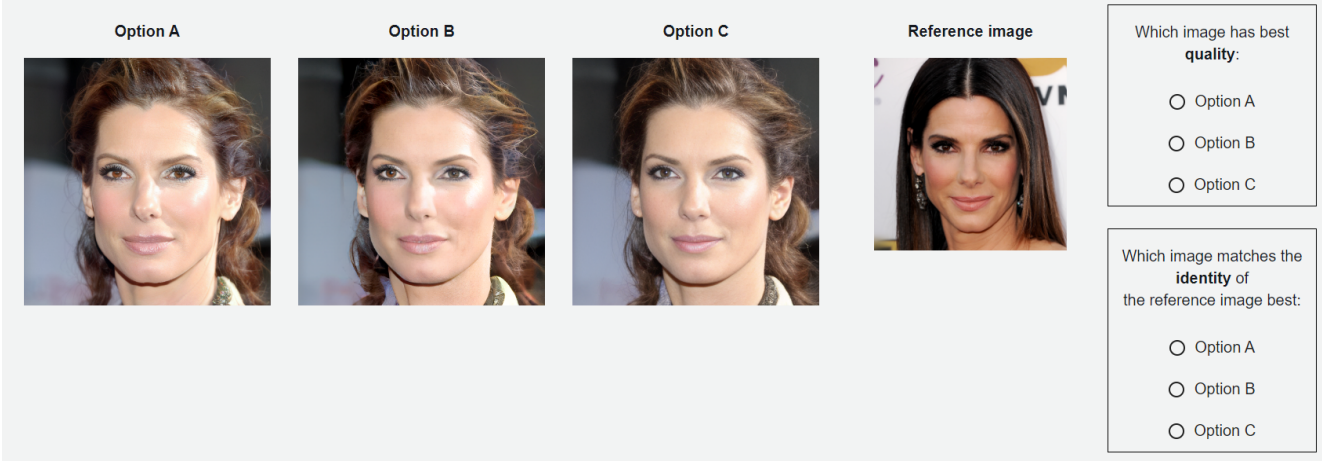


Figure 11. User interface used in the user study.

study. The instructions detail the two different tasks and how they should be evaluated.

Amazon Mechanical Turk is used for the study. We follow principles from [30]. We filter users based on the Master certificate to ensure quality annotations. For each task we pay \$ 0.04 as suggested in [30].

Personalized Model Additional Experiments

In this section we detail the full experimental settings and conduct additional experiments of hyperparameters for the personalized model. In all experiments, excluding the parameter to be studied other hyperparameters are kept constant. With further fine-tuning of hyperparameters, results for specific individuals and inputs can be improved.

Settings Followed by community findings that prompts can improve quality of the restored image, we use both a positive and a negative prompt. For the positive prompt we use *"a Photo of *, masterpiece, best quality, realistic, very clear, professional"* and for the negative prompt we use *"3d, cartoon, anime, sketches, worst quality, low quality"*. We note that including semantic changes in the prompt like *"red hair"* does not have an effect. This is due to the restoration blocks fusing the low-quality image with the denoised image directly. This is in line with the goal of the paper, as it is a restoration method, not an editing method.

For the classifier-free guidance value we set 4 as a default for all experiments. Standard DDPM [16] sampling is used with 200 steps as in StableSR [38]. As the personalization fine-tuning approach is about learning a single identity and not multiple parts of an identity, we find that not using the 50% random crops improves the results slightly. For the baseline method DR2 + SPAR [41] we empirically ex-

perimented with several hyperparameters values of N and τ that are crucial for the performance of the method. N is a downsampling factor and τ is the output step after which generation is started. We set $N = 8$ and $\tau = 40$ as we found it performed the best across different levels of degradations. For LMSE (Landmark MSE) [47] was used to obtain landmarks. In cases where landmarks could not be found due to the image being severely degraded the MSE was set to 128. Similarly in cases where the MSE was for an image was more than 128 it was capped to 128 to avoid outliers due to numerical errors or other errors.

Degradations During testing we synthesized a light and a heavy degradation to better evaluate our algorithm in different situations. During training we use the heavy setting. We use the settings from StableSR as a base and modify them. To better suit for real-world applications we include motion and median blur, as well as adding ISP (Image Signal Processing) noise [44].

To ensure our method works in less severe cases, we also include a light partition during testing. Here, we only include a first-order noise similar to CodeFormer.

The light portion follows:

$$I_D = \{[(I \otimes k_\sigma) \downarrow_r + n_\delta]_{\text{JPEG}_q}\} \uparrow_r, \quad (8)$$

where k_σ is Gaussian blur kernel, \downarrow_r and \uparrow_r are the downsampling and upsampling operators, n_δ additive Gaussian noise and $[\cdot]_{\text{JPEG}_q}$ is JPEG compression. We sample uniformly σ , r , δ and q from $[0.1, 10]$, $[1, 4]$, $[0, 2]$ and $[30, 100]$, respectively. The additive Gaussian noise has a probability of 40% and downsampling a probability of 70%, while filtering and JPEG compression occur always.

The heavy portion first applies ISP model [44] with a 50% probability, followed by motion and median blur with

5% and 10% probabilities. Next, we use equation 8 and the same settings except, r and δ are chosen from $[1, 10]$ and $[0, 15]$, respectively, followed by a sinc filter [38]. Finally, equation 8 is applied a second time with a 90% probability.

Classifier-Free Guidance Value To further emphasize the conditional element, CFG [15] can be used to guide the denoising process. As mentioned earlier, we use a negative prompt instead of a null one. The formula is given by

$$\tilde{X} = X + \lambda_{cfg}(X(p_{pos}, I_{LQ}) - X(p_{neg}, I_{LQ})), \quad (9)$$

where p_{neg} and p_{pos} correspond to the positive and negative prompts. We also experimented with null conditioning the low-quality image

$$\tilde{X} = X + \lambda_{cfg}(X(p_{pos}, I_{LQ}) - X(p_{neg}, \emptyset)), \quad (10)$$

but found the results to be of lower-quality, as emphasizing the low-quality image may exaggerate blurry features.

We experiment using Eq. (9) with different CFG values λ_{cfg} in Fig. 12 and note that $\lambda_{cfg} = 1$ corresponds to not using guidance at all. It can be seen that a higher λ_{cfg} can oversaturate, as in the top row. In the lower row, a low λ_{cfg} loses identity features, whereas in the top row it is more subtle. From our experiments we observe that different identities behave differently with different λ_{cfg} . A common value in text-to-image applications is $\lambda_{cfg} = 7.5$, but to avoid saturation we default to $\lambda_{cfg} = 4$ in all of our other experiments.

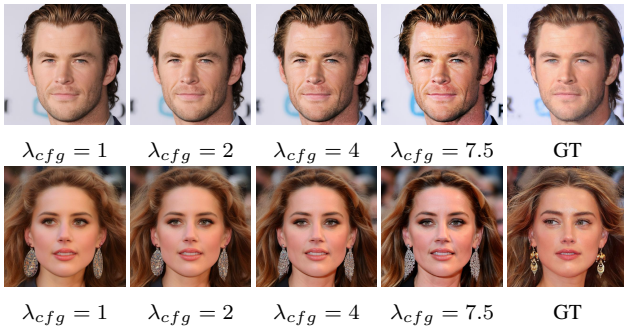


Figure 12. Experiments with different classifier-free guidance values.

Controlling Identity The used personalization technique consists of two parts. 1) a learnable text-embedding and 2. image cross-attention. We experiment with different values of λ_{att} , which controls the weight of the cross-attention layers, in Fig. 13. The sample with $\lambda_{att} = 0$ corresponds to only using the learnable text-embedding. We can see that it contains some identity at a high-level but is missing details such as wrinkles and dip in the chin. With increasing λ_{att} the identity features become more prominent, even to

a degree of exaggeration. Similar to CFG values, we have observed that for different individuals and depending on the noise levels of the input, λ_{att} acts differently. We chose $\lambda_{att} = 1$ as a default value, although in some cases, like this sample, the optimal results can be something different.

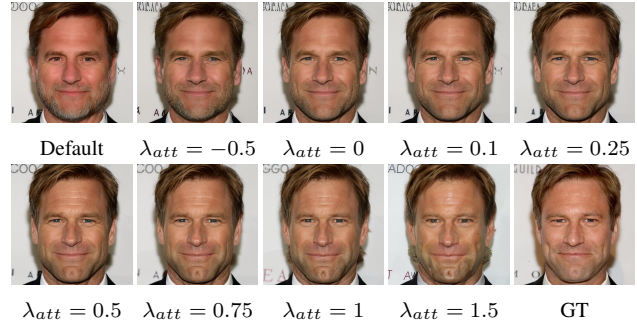


Figure 13. Controlling identity. The default corresponds to non-personalized output. Samples with λ_{att} , use the personalized token in the prompt.

Number of Reference Images In Fig. 14 we experiment with how many reference images are required to accurately capture the identity. With $n_{img} = 0$, i.e. no personalization, high-level features matching the input can be observed. With just one reference image, the eyes, eyebrows and other finer details start to appear. We default to using $n_{img} = 5$ as it often performs sufficiently and the addition of more images has less noticeable effect. For some individuals we found that even three images can be sufficient, but it should be noted that the similarities between input image and the reference images affect the results.

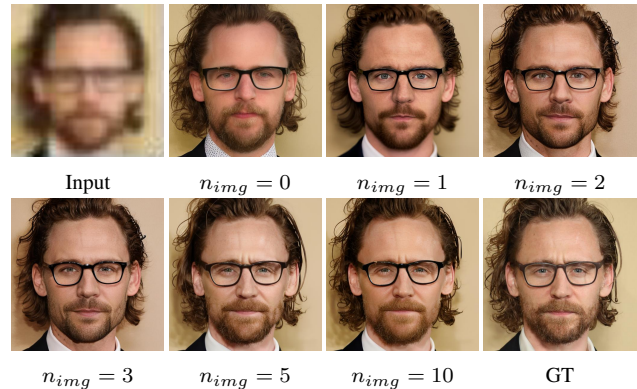


Figure 14. Number of images used for personalization. $n_{img} = 0$ refers to no personalization.

Randomness with Different Seeds Diffusion models are stochastic and notorious for unsatisfactory results with different random initializations. Figure 15 contains results for

an image with light and heavy degradations with four different seeds. For the light portion, the outputs tend to be mostly similar with small differences like skin texture. With the heavy portion, there are noticeable differences in the mouth, eyes and colors, although the identity is kept the same. Interestingly the background logo and text deviate largely, as they are not part of the learned personalization.

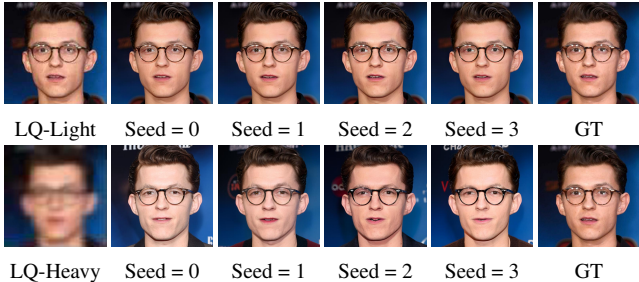


Figure 15. Random seed effect.

Additional Qualitative Results Here we provide additional results on the light, heavy and real portions of the Celeb-Ref [26] dataset. From Fig. 17 row three, we can see that the DMDNet is able to better preserve the identity compared to CodeFormer, but compared to ours it is still missing fine-grained details such as the notch in the chin. Despite achieving good results with light degradations, DMDNet struggles with the heavy and real degradations in Figs. 18 and 19. Although DR2 provides poor results in several cases, it works well on row 4 of Fig. 18.

Despite the input being very noisy and small in size, our result is faithful with the identity, while codeformer struggles due to requiring alignment. Figure 16 contains a qualitative comparison between different personalization techniques and more results are provided in Figs. 20 and 21.

Additional Quantitative Results To complete the quantitative results of heavy portion from Tab. 1, the results of light and real portions are presented.

Table 3 tabulates the results for the real portion. As no GT is available, we only use MUSIQ [20] and ID [7] as metrics. For the ID we use a reference image of the same person. As can be seen from the results, the ID metric drops significantly compared to the heavy portion, where ID used GT image. Despite this the rankings of the results remain similar with ours as first and DMDNet and CodeFormer being close with similar results and DR2 achieving the lowest due to blurry results. Base Model + DreamBooth [33] achieves the best result in ID which is likely due to overfitting to the identity, with poor restoration results. Table 4 presents results for the light partition. Our method is consistently among the second best performers, although the differences between the methods are minor.

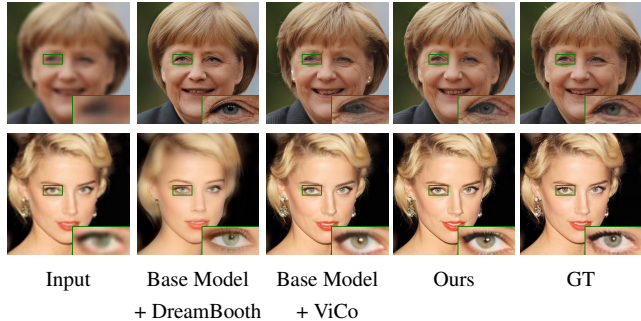


Figure 16. Results using different personalization techniques combined with a base restoration model. DreamBooth [33] is not able to capture all the details and can result in poor-quality images. ViCo is better able to capture most details, but can still result in blurry images. Ours is able to capture fine-grained details without hurting the restoration performance of the Base Model. Zoom in for best view.

Table 3. Quantitative results for the real portion of the data. Red indicates the best and blue indicates the second best

Methods	Ref	MUSIQ \uparrow	*ID \uparrow
Input		24.84	20.37
StableSR [38]		51.59	23.39
Base Model		60.27	24.29
Base Model + DreamBooth	✓	55.31	29.78
Base Model + ViCo	✓	57.67	24.71
DMDNet [26]	✓	58.36	22.29
DR2 [41]		29.18	18.38
CodeFormer [48]		44.60	22.90
PFSStorer (Ours)	✓	60.11	25.01

* Compare with a reference image.

Value of Learnable γ after training Each layer l has vector γ^l with the size depending on the layer hidden dimension. The values of the mean of the vector for each layer is around 0.2 and 0.5. The higher importance of 0.5 values is from the middle of the UNet layers, where the resolution is lowest and the lower values of 0.2 at the higher resolution layers.

Non-Personalized Base Model Experiments

In this section we cover the training details and results with the Base Model without personalization. The model is a pre-trained StableSR [38] without any modifications to the architecture. The personalized models all use the fine-tuned Base Model described in this section as their starting point.

Training The training is performed on a facial dataset FFHQ [18], which contains 70,000 facial images in the resolution of 1024×1024 . 50% of the data is resized randomly to 512×512 and the other 50% are taken as ran-

Table 4. Quantitative results for the light portion of the data. **Red** indicates the best and **blue** indicates the second best

Methods	Ref	PSNR \uparrow	SSIM \uparrow	LPIPS \downarrow	MUSIQ \uparrow	LMSE \downarrow	ID \uparrow
Input		22.56	0.719	0.615	58.83	9.74	21.85
StableSR		27.18	0.767	0.337	62.96	5.73	70.62
Base Model		27.72	0.767	0.318	64.16	4.93	72.43
Base Model + DreamBooth	✓	24.77	0.721	0.419	62.01	14.29	62.57
Base Model + ViCo	✓	27.58	0.765	0.325	63.04	4.88	73.26
DMDNet [26]	✓	27.72	0.780	0.312	63.07	6.43	72.66
DR2 [41]		22.17	0.701	0.449	47.36	13.13	30.01
CodeFormer [48]		27.19	0.759	0.293	66.00	5.91	69.13
PFStorer (Ours)	✓	27.71	0.767	0.309	63.31	4.79	75.39
GT		∞	1	0	62.37	0	100

dom crops of the same resolution. Fine-tuning is performed for 12 epochs. At this moment the personalization adapter is not attached to the model. We synthesize training data in the same manner as the personalized model with the heavy degradation.

Qualitative Results For qualitative results on synthetic degradation on CelebA-Test split [27], see Fig. 22. The synthetic degradation for CelebA-Test is obtained from [40]. Compared to CodeFormer [48] our method is able to generate more fine-grained details, while being more faithful to the low-quality image, *e.g.*, the color of facial hair on top. Results from real-world datasets, LFW [17], WebPhoto [40] and Wider-Test [48] are shown in Fig. 23. In LFW, which contains less severe degradations, compared to CodeFormer our method is able to generate more details with sharper textures. Our method struggles with WebPhoto, as it contains old images with scratches, color degradation and other untypical degradations. With severe degradation on Wider-Test, our method is able to generate realistic images, while CodeFormer struggles with artifacts.

Quantitative Results We provide quantitative results with standard metrics. Table 5 tabulates results from CelebA-Test, where the results are taken from [40], except for CodeFormer and ours. In most of the metrics the results are similar between GFP-GAN, CodeFormer and ours. In the real-world datasets, Tab. 6, our method obtains the best FID for LFW and WIDER.

Table 5. Quantitative results for CelebA-Test with non-personalized model. **Red** indicates the best and **blue** indicates the second best

Methods	PSNR \uparrow	SSIM \uparrow	LPIPS \downarrow	MUSIQ \uparrow	FID \downarrow	ID \uparrow
Input	25.35	0.684	0.486	58.83	143.98	52.06
DFDNet	23.68	0.662	0.4341	N/A	59.08	59.69
PULSE	21.61	0.620	0.4851	N/A	67.56	30.45
GFP-GAN	25.08	0.677	0.3646	N/A	42.62	65.40
CodeFormer	26.77	0.719	0.343	66.54	52.44	62.73
Base Model	26.03	0.680	0.392	66.57	40.36	63.89
GT	∞	1	0	63.43	43.43	1

Table 6. Quantitative results for real-world datasets with non-personalized model. **Red** indicates the best and **blue** indicates the second best

Dataset Degradation Methods	LFW-Test mild		WebPhoto-Test medium		WIDER-Test heavy	
	FID \downarrow	MUSIQ \uparrow	FID \downarrow	MUSIQ \uparrow	FID \downarrow	MUSIQ \uparrow
Input	137.56	25.05	170.11	19.24	202.06	15.57
PULSE	64.86	66.98	86.45	66.57	73.59	65.36
DFDNet	62.57	67.95	100.68	63.81	57.84	59.34
GFP-GAN [40]	49.96	68.95	87.35	68.04	40.59	68.26
CodeFormer [48]	52.02	71.43	78.87	70.51	39.06	69.31
Base Model	44.11	66.57	80.90	62.69	34.72	63.91
Light degradation	44.02	62.69	84.81	57.64	82.93	51.66

Ablation: Heavy Degradation We show that with more complex degradations the method is able to perform better in cases with severe degradation. The results are tabulated in bottom of Tab. 6. *Base Model* uses the heavy degradation, where as the *Light degradation* does not. For LFW, which has relatively mild degradations, the performance between Base Model and simple degradation does not change drastically as expected. However, for WIDER-Test we can see a large difference as the FID more than doubles from 34.72 to 82.93, meaning a significant decrease in quality. Using heavy degradation results in higher quality outputs under severe degradation, while having minimal effect on mild cases.

Societal Impact

Machine learning models can learn biases from their datasets. We show that our model is capable of working with different ethnicities and skin tones, while acknowledging that the testing is limited. We also note that since our model is built upon previous models, it inherits any biases these models may contain. To avoid misunderstanding of the capabilities of our models, *e.g.*, using it for enhancing security footage for criminal investigations, we have shown the limitations in experiments and emphasize that the identity of the restored individual needs to be known beforehand. Malicious users may want to mislead viewers with generated images, which is a common common issue with existing similar methods. However, recent approaches in detecting fake imagery are improving rapidly.

Privacy and Image Copyrights In this paper we showcase several pictures of individuals. Several images are from the publicly available Celeb-Ref dataset [26]. Images shown from the collected 20 image dataset are of well-known celebrities and are under a Creative Commons license. Real world images not part of the collected dataset are under public domain or a Creative Commons license.



Figure 17. Qualitative comparison with state-of-the-art restoration models on Celeb-Ref dataset [26] with synthetic light degradation.

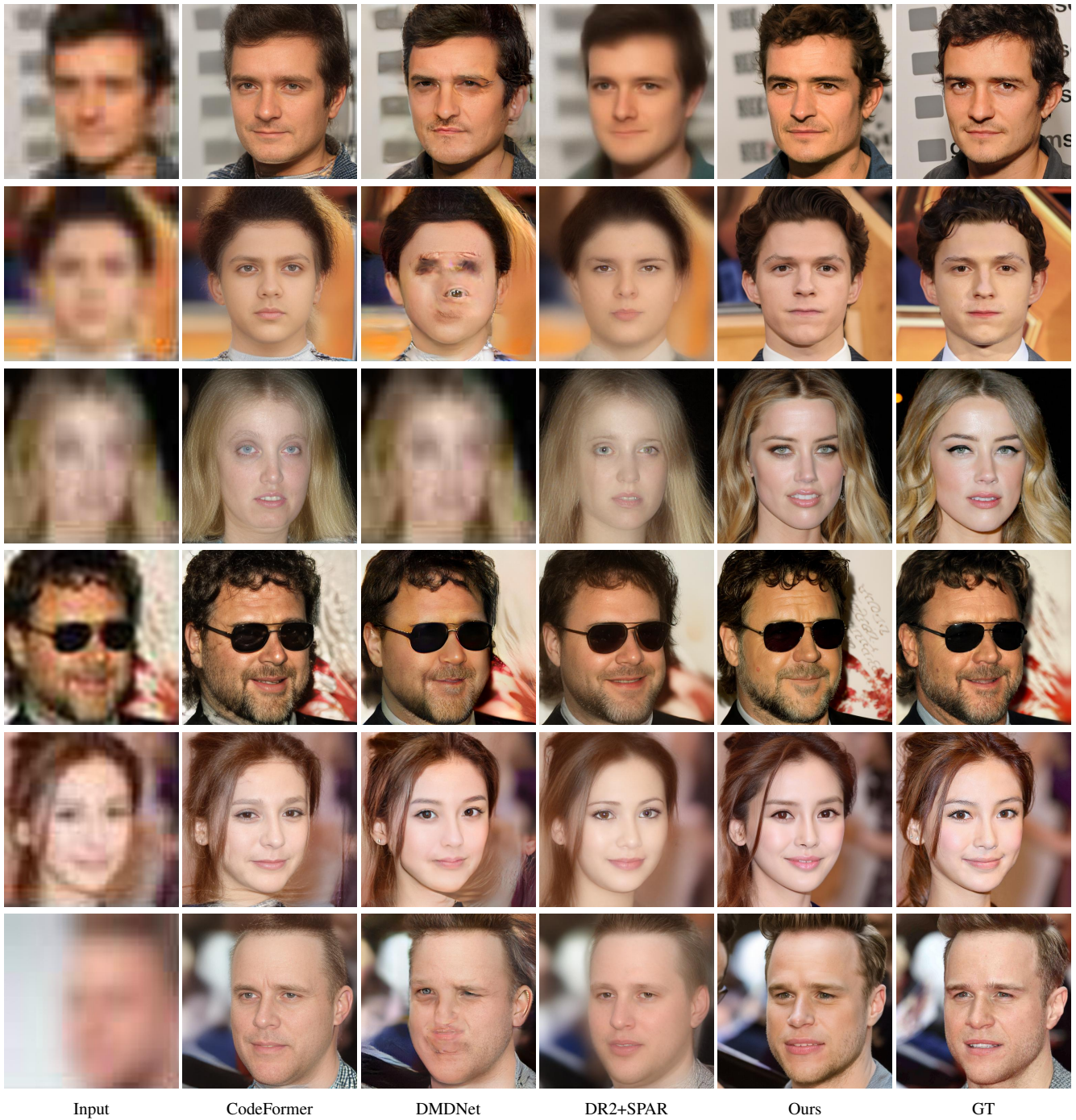


Figure 18. Qualitative comparison with state-of-the-art restoration models on Celeb-Ref dataset [26] with synthetic heavy degradation.



Figure 19. Qualitative comparison with state-of-the-art restoration models on Celeb-Ref dataset [26] with real degradation.

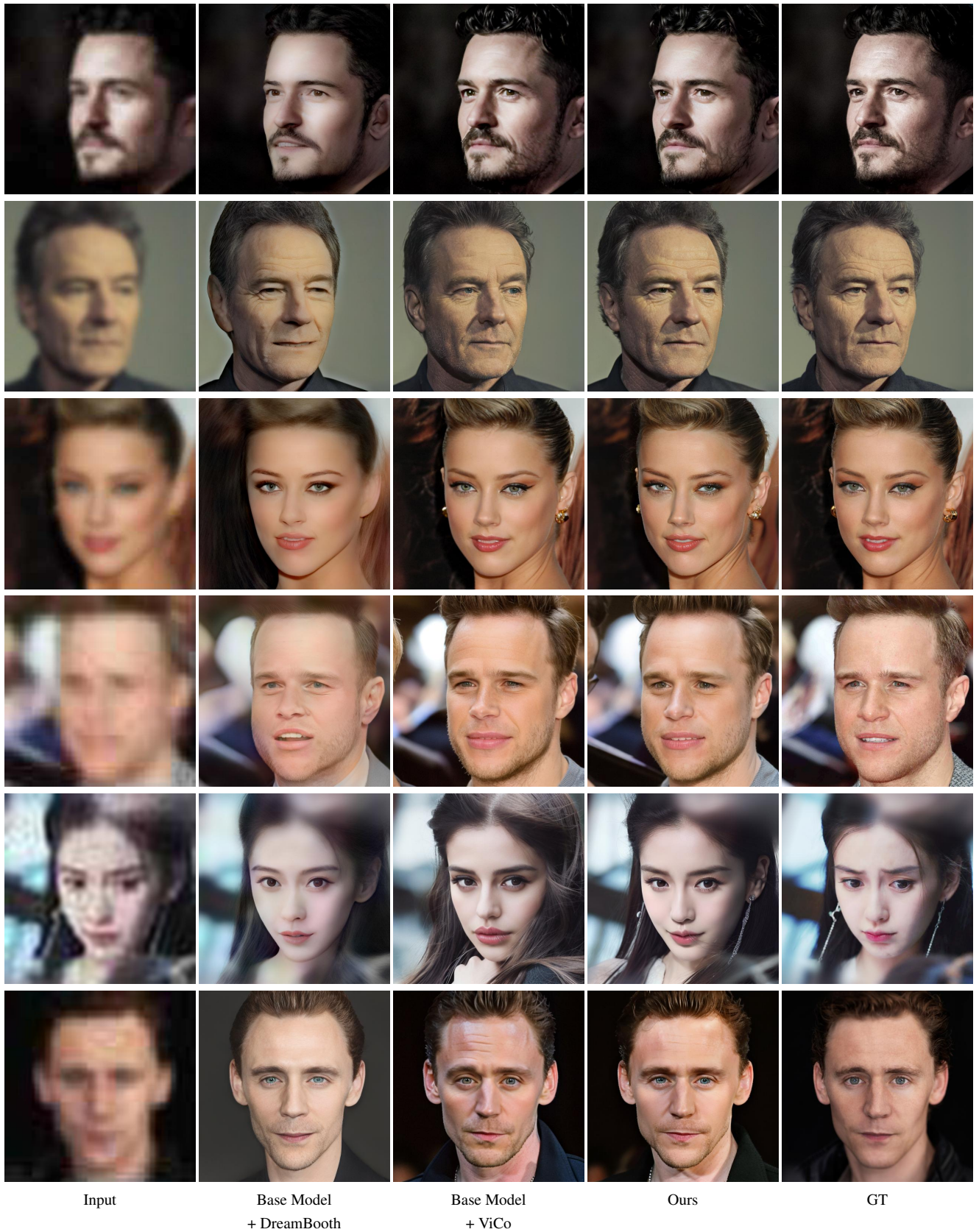


Figure 20. Results using different personalization techniques combined with a base restoration model with heavy degradation.

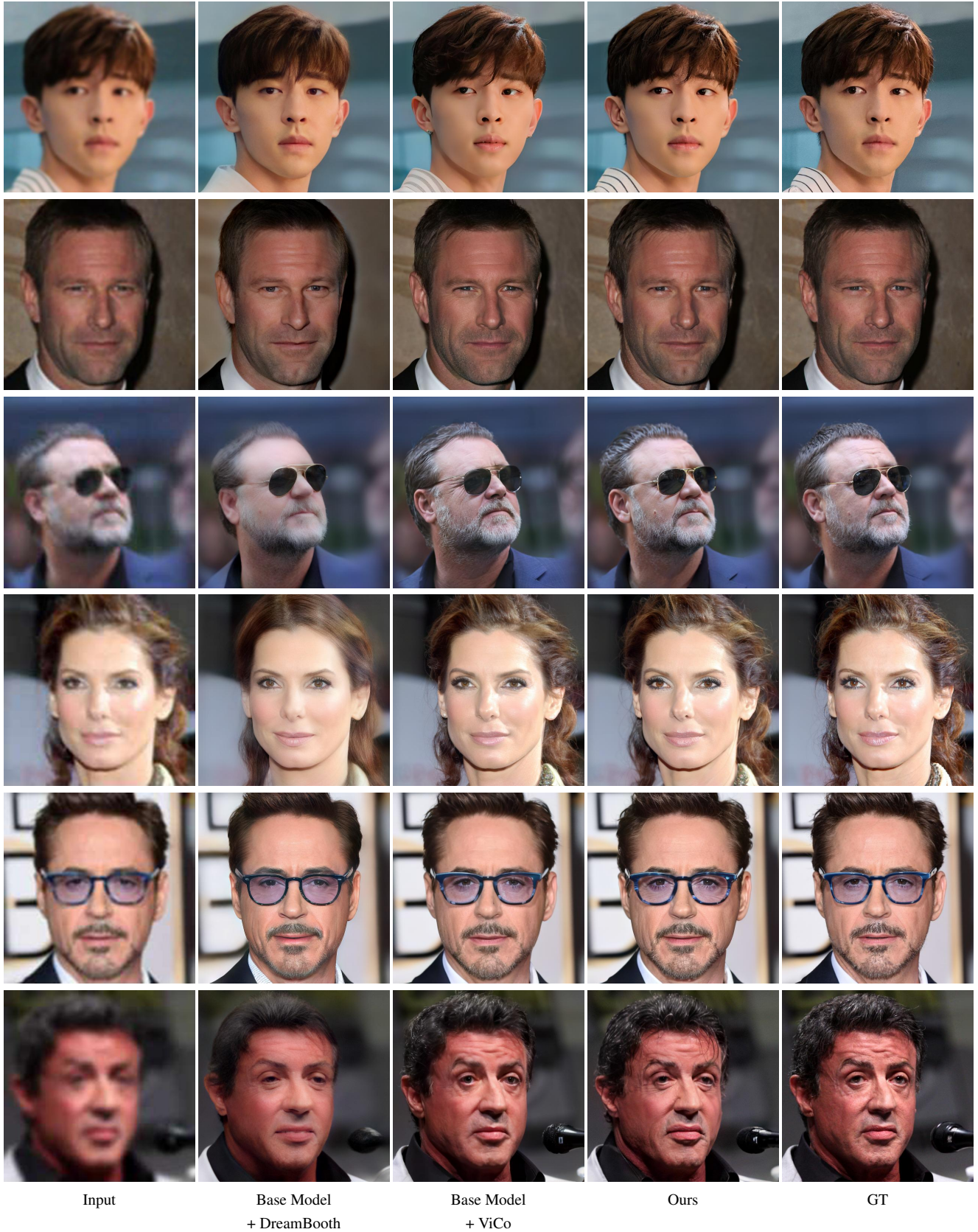


Figure 21. Results using different personalization techniques combined with a base restoration model with light degradation.

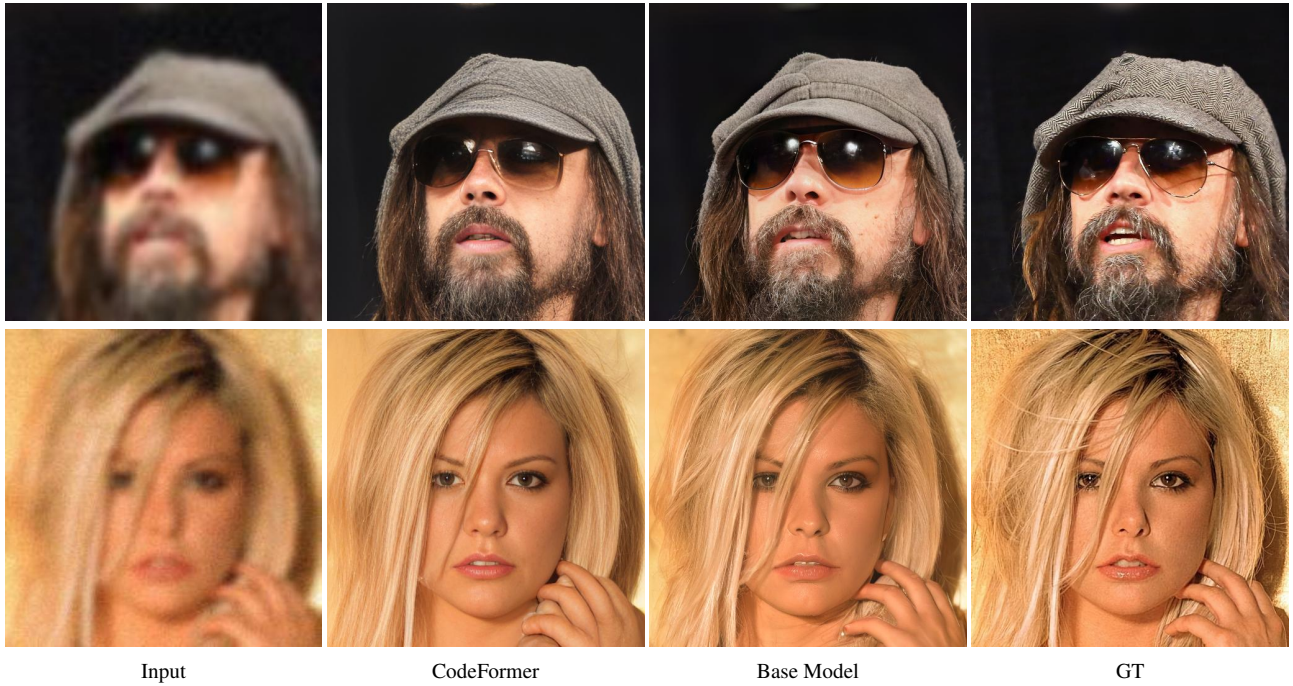


Figure 22. Qualitative comparison with state-of-the-art restoration models on CelebA-Test [27] with synthetic degradation.



Figure 23. Qualitative comparison with state-of-the-art restoration models on LFW [17], WebPhoto [40] and Wider-Test [48].